Research article

Protein expression profiling in rat hippocampus after focal cerebral ischemia injury

Lichan He[1], Rui He[1], Ruihua Liang[1], Yi Li[1], Xiaoqiang Li[1], Chuqiao Li[1], Suping Zhang[1,*]

[1] *Department of Neurology, Guangzhou Red Cross Hospital, Medical College, Jinan University, No. 396 Tongfu Zhong Road, Guangzhou 510220, China*

***Correspondence**: supingzhang@yeah.net (Suping Zhang)

https://doi.org/10.31083/JIN-170047

Abstract

The aim in this study was to explore protein expression profiles in the rat hippocampus after induction of focal ischemia injury. Forty male Sprague Dawley rats were randomly divided into four equal groups after ischemia injury surgery: Control, Day 3, Day 7, and Day 14. Focal cortical ischemia was induced in thirty rats by photothrombosis of cortical microvessels. After surgery, the induction of ischemia was confirmed by infarct size measurement using staining by 2, 3, 5-triphenyltetrazolium chloride. To identify the differential expression of proteins between the diseased and control sides of the hippocampus, a comparative proteome analysis was performed using isobaric tags for relative or absolute quantification coupled with 2D liquid chromatography-tandem mass spectrometry analysis. 4,081 proteins were identified, 260 of which were non-redundant and showed differential expression between the three surgery groups and the control. Hierarchical cluster analysis indicated that the three surgical groups had markedly different expression patterns of these 260 proteins, including 160 upregulated and 80 downregulated proteins. A gene ontology analysis revealed 4,944 terms, among which myelin sheath and cell junction were the two most enriched items. In kyoto encyclopedia of genes and genomes database pathway analysis, ribosome was the most abundant item. A Venn diagram showing the overlap of 25 of the differentially expressed proteins quantified from the four groups and results from the kyoto encyclopedia of genes and genomes pathway analysis suggested that Epstein-Barr virus infection was the most abundant item. From the protein-protein interaction network, a total of 223 interactive proteins were predicted and used to construct a network. In conclusion, myelin sheath, cell junction, and Epstein–Barr virus infection were implicated in focal ischemia injury. Vimentin and albumin may be important proteins involved in focal ischemia injury.

Keywords

Focal ischemia injury; isobaric tags for relative or absolute quantification; gene ontology analysis; kyoto encyclopedia of genes and genomes pathway; proteomics; rat model

Submitted: June 21, 2017; **Accepted:** September 11, 2017

1. Introduction

Cerebrovascular disease is the third most common cause of death worldwide, of which 60%–70% is ischemic cerebrovascular disease (ischemic stroke) [1]. Recent advances in the epidemiology of cerebral ischemia suggest a strong association between vascular factors predisposing to cerebrovascular disease [2, 3], cerebrovascular diseases are also the second leading cause of dementia [4]. Studies have shown there are several risk factors for ischemic cerebrovascular disease, including high blood pressure, ischemic heart disease, hyperlipidemia, diabetes mellitus, obesity, and smoking [5–8]. Stroke can lead to irrevocable damage to brain regions that play an important role in memory function, including the thalamus and the thalamocortical projections [9] and has also been shown to effectively promote Aβ deposition, which could result in cognitive decline [10].

Proteomics is the large-scale study of proteins and employs techniques to identify complete protein complements of an expressed genome, thereby providing a macroscopic view of which proteins are expressed and present under different growth conditions [11]. Generally, proteomics is an ideal method for the identification of differentially expressed proteins, in order to ascertain the actual activity of metabolic reactions and/or regulatory cascades [12]. Isobaric tags for relative and absolute quantification (iTRAQ) have been widely used for biomarker discovery [13, 14] and is a technology that has also been widely used for the identification and relative quantification of proteins and peptides. The liquid chromatography–mass spectrometry (LC-MS) and liquid chromatography-tandem mass spectrometry (LC-MS/MS) methods were developed for the simultaneous analysis of differently expressed proteins and peptides [15]. iTRAQ is conceptually elegant, since peptides are labelled at the N-terminus and at the ε-side chain of lysines [16–18]. Moreover, iTRAQ is robust, due to its stable N-hydroxysuccinimide (NHS) ester chemistry [13]. The ability to simultaneously analyze multiple samples has proven popular, and iTRAQ now has applicability across diverse mass spectrometry platforms, including quadrupole time-of flight (Q-ToF), ion trap, and others [19, 20]. At this point, iTRAQ has shown many advantages compared with other conventional proteomic techniques. For example, it enhances the use of robust bioinformatic tools [21] and statistical analysis [22]. In a previous study, ten hyper-phosphorylated Lys-Ser-Pro sites were identified on the C-terminal tail domain of neuronal intermediate filament proteins, with greater phosphorylation abundance in the Alzheimer's brain compared with the control brain, as assessed by iTRAQ quantitative

phosphoproteomic analysis [23].

This work reports a set of differentially expressed proteins in the hippocampus of Sprague Dawley (SD) rats after focal ischemia injury.

2. Materials and methods

2.1. Ethics statement

The animal study was approved by the Animal Ethics Committee of the Guangzhou Red Cross Hospital, China. All animals were carefully handled in compliance with established guidelines.

2.2. Ischemia injury in rats

Forty male SD rats (weight approximately 100 ± 20 *g*, four–five weeks old) were supplied by the Animal Center of Jinan University (Guangzhou, China). Rats were housed in a temperature and humidity-controlled room on a 12/12 hour light/dark cycle and food and water were freely available. After one week, all rats were randomly divided into four groups (10 rats per group): Control, Day 3, Day 7, and Day 14 after ischemia injury surgery. Focal cortical ischemia was generated by photothrombosis of the cortical microvessels as described in a previous study [24]. Briefly, rats were anesthetized and body temperature maintained at 37 ± 0.5°C by heat pad. The rat skull was exposed at 0.5 mm anterior and 3.7 mm lateral from the bregma, the skull was laser illuminated at a wavelength of 561 nm, eight mm diameter for 10–15 min, after infusion with Rose Bengal (RB, 50 mg/kg body weight, Sigma-Aldrich, CA, USA) which was dissolved in normal saline into the right femoral vein for two minutes [24]. The scalp was sutured and rats were allowed to wake before being returned to their cages. A sham control group received the same vein injection of Rose Bengal and the same surgery but without laser exposure to avoid any photochemical reaction. A schematic diagram of this surgery is given in Fig. 1A. At scheduled time points, rats were sacrificed and their brains removed and immersed overnight in a fixative solution. The hippocampi were dissected out under microscopy, frozen immediately in liquid nitrogen, and stored at −80°C until required.

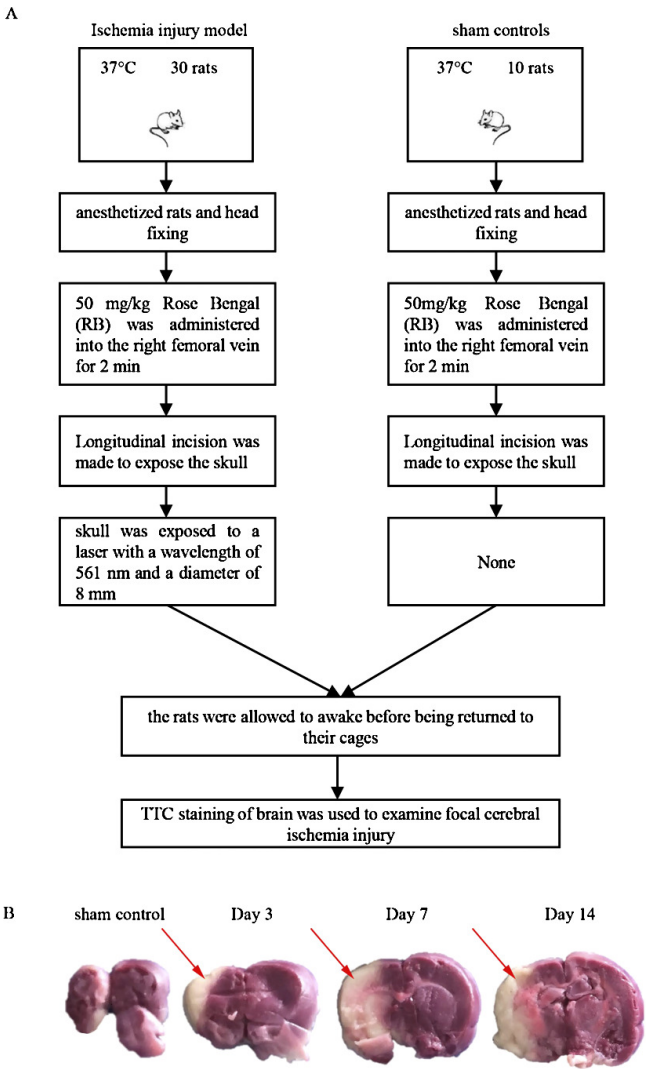

Fig. 1. (A) A schematic diagram showing how photothrombosis induces focal ischemic injury in rats. (B) Lesion areas visualized by TTC staining. TTC staining colors: red–viable tissue, white–ischemic tissue lesions.

2.3. Measuring the ischemic lesion

Ischemic lesion were measured after surgery at days 3, 7, and 14. Rats were anesthetized with carbon dioxide and sacrificed with a rat guillotine. Brains were immediately obtained, placed into a rat brain matrix (RBM-4000, ASI Instrument, USA), and frozen at −20°C for 20 min. The brain was then cut into 2-mm blocks and immersed in PBS at room temperature. Each slice was then incubated in a solution of 2% 2,3,5-triphenyltetrazolium hydrochloride (TTC) (Sigma-Aldrich, St. Louis, MO, USA) and maintained at 37°C in a heater in the dark for 30 min, before excess TTC was drained and slices were fixed with 4% poly (tetrafluoroethylene-co-perfluoropropyl vinyl ether) (PFA) for 20 min. Infarcted brain tissue remained unstained (white), whereas normal tissue stained red.

2.4. Protein extraction, digestion, and iTRAQ labeling

Proteins and three biological replicates were collected from each group using the phenol extraction method [25]. Briefly, about 200 μg protein samples were mixed into 30 μL STD buffer, the mixture was incubated at 100°C for five minutes and cooled to about 25°C. The solution was then diluted with a 200 μL UA buffer and a 30 kDa ultrafiltration and centrifuged at 14,000 *g* for 15 min at room temperature. These steps were repeated with 100 μL UA buffer added to the sediment and dark incubated for about 20 min. Samples were then centrifuged at 12,000 *g* for 10 min. Filters were washed with 100 μL UA buffer and 100 μL DS buffer, then 2 μg trypsin (Promega, USA) in 40 μL DS buffer, which was added to each filter. Samples with other buffers were incubated overnight at 37°C and the resulting peptides were processed by centrifugation. Filters were rinsed with 40 μL 10 × DS buffer, recentrifuged, and finally the peptide content was tested for spectral density with UV light at 280 nm. About 100 μg of peptides from each treatment group were labeled with iTRAQ reagents following the manufacturer's instructions (Applied Biosystems, CA, USA).

2.5. Separation of peptides and mass spectrometric analysis

Peptides were purified from excess labeling reagent by High Performance Liquid Chromatography (HPLC) (Shimadzu Corporation,

Japan) prior to the mass spectrometric analysis. Labeled samples were dried and then diluted with 20-fold cation exchange binding buffer A (containing 10 mM KH_2 PO_4, at pH 3.0, and 25% ACN). The labeled samples were then separated into ten fractions by gradient elution in a poly-sulfoethyl 4.6 $\times$ 100 mm A column (5 m, 200 A; Poly LC, Columbia, MD, USA) [26].

2.6. *Annotation and functional enrichment analysis of differentially expression proteins*

The heat map was generated using Heatmap V2.0 (R-package). The biological processes, molecular functions, and cellular components of the identified differentially expressed proteins were examined with KOBAS software to perform gene ontology (GO) annotation (http://kobas.cbi.pku.edu.cn/home.do) [27]. The GO enrichment analysis of the differentially expressed proteins was implemented with WEGO software (http://wego.genomics.org.cn/cgi-bin/wego/index.pl), in which the gene length bias was corrected. A corrected p value < 0.05 was chosen to include as many items as possible [28]. Kyoto encyclopedia of genes and genomes (KEGG) is a database resource for the analysis of high-level gene functions and biological gene systems (http://www.genome.jp/kegg/) [29]. Cluster Profiler software (R-package) was employed to test the statistical enrichment of differentially expressed proteins in KEGG pathways. A P value < 0.05 was also chosen so as to include as many items as possible.

2.7. *Protein–protein interaction (PPI) network construction*

A PPI network analysis provides new insights into protein function. A PPI network was constructed to further analyze the function of 25 common differentially expressed proteins. The Search Tool for the Retrieval of Interacting Genes/Proteins (STRING) (https://string-db.org/) provides the information for both predicted interactions. With this tool, differentially expressed protein pairs with significant interactions (combined score > 0.9) were identified and used for the construction of the PPI network, which in turn was visualized using Cytoscape (http://cytoscape.org/).

3. Results

3.1. *Ischemic lesion in rats after surgery*

The brain infarct size after surgery was evaluated by TTC assay. Infarcted brain tissue was white, whereas the normal tissue was stained red. No infarct damage was found in control rats (Fig. 1B), while infarct regions were identified in Day 3 rats. Furthermore, the infarct size in Day 7 rats was slightly bigger than that of the Day 3 group, which was also the case for Day 14 rats (Fig. 1B). These results suggest that brain ischemia and ischemic damage was successfully induced in rats following focal cortical ischemia surgery.

3.2. *Protein expression profiles in the hippocampus after ischemia injury*

A total of 4,081 peptides from the unique trypsin-digested proteins of all four groups were identified. 260 non-redundant proteins were identified with significantly differential expression that was more common in rats from Day 3, 7, and 14 groups than in the control group (Fig. 2). In a comparison of Day 3 and control groups, 90 proteins were markedly upregulated and 170 were markedly downregulated. In a comparison of the control and Day 7 group, 83 proteins were markedly upregulated and 167 were markedly downregulated. The comparison of the Day 14 and the control groups was even more dramatic, with 98 markedly upregulated and 162 markedly downregulated proteins. Hierarchical cluster analysis revealed that Day 3, 7, and 14 groups had clearly different expression patterns among the 260 identified proteins, of which 160 were upregulated in the three different groups when compared to the control (Fig. 2) and 80 proteins were downregulated. Sample clustering results indicated that protein expression patterns in the Day 3, 7, and 14 groups were more similar to each other than to those of the control group. 34.6%, 31.9%, and 37.7% of proteins were downregulated in the three different groups, while 65.4%, 64.2%, and 62.3% of proteins were upregulated, respectively, when compared to controls.

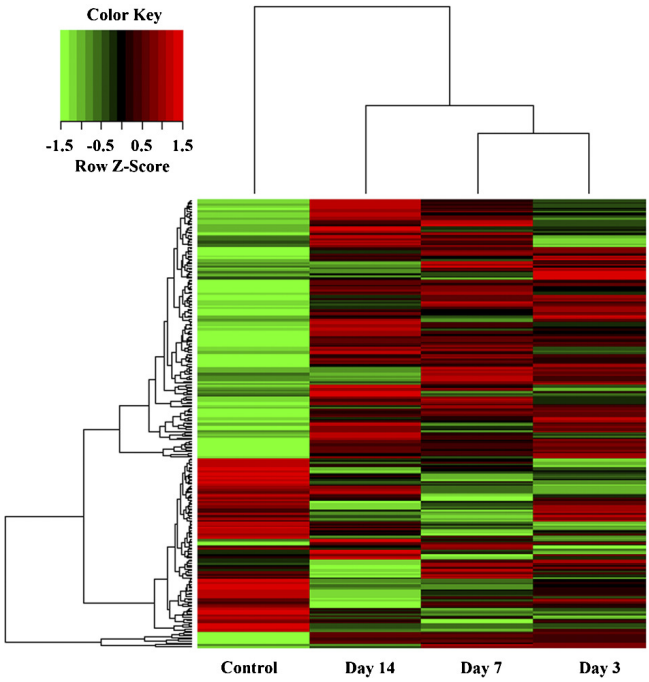

Fig. 2. Hierarchical clustering of 260 differentially expressed proteins. Four main protein expression patterns were identified: the control was the protein expression atlas occurring within the first day after surgical simulation of the healthy side of the hippocampus; Day 3, 7, and 14 were the protein expression atlases occurring on the third, seventh, and fourteenth day, respectively, after surgical simulation of the diseased side of the hippocampus. Increasing red color indicates an increasing protein expression level.

3.3. *GO and KEGG pathway analysis of 260 differentially expressed proteins*

GO annotation and enrichment analysis of 260 differentially expressed proteins that were more common in the three groups than the control were implemented with KOBAS and WEGO software. All GO terms with corrected P values less than 0.05 were considered to be significantly enriched. There were 4,944 GO items harvested in this study. Myelin sheath (GO: 0043209) and cell junction (GO: 0030054) were the two most enriched items. The distribution bar charts of the biological processes, cellular components, and molecular functions are shown in Fig. 3. From the perspective of biological processes, those of cellular processes, metabolic processes, and pigmentation were the top three significantly enriched terms. In the

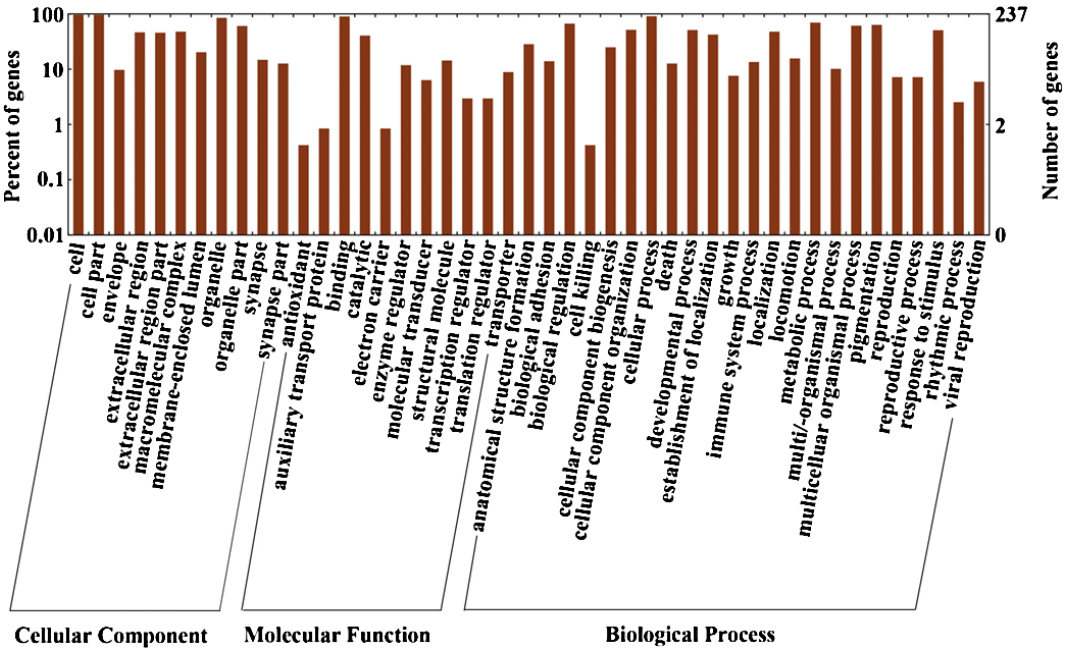

Fig. 3. Gene ontology(GO) enrichment analysis of the 260 differentially expressed proteins identified in this study.

molecular function category, binding, catalytic, and structural molecular functions were the top three. In the cellular component category, cell and cell parts were the top two significantly over-represented terms.

KOBAS software (http://www.genome.jp/kegg/) was employed to test the statistical enrichment of differentially expressed proteins using KEGG pathways. In this study, 260 differentially expressed proteins involved 220 pathways. Fig. 4 shows the results of the KEGG pathway enrichment, clearly showing ribosome pathways as the top enriched term (Fig. 4). In addition, 12 differentially expressed proteins identified in this study were identified as participants in ribosomal pathways. Moreover, it is noteworthy that proximal tubule bicarbonate reclamation, endocrine and other factor-regulated calcium reabsorption, and regulation of actin cytoskeleton and synaptic vesicle cycle were also significantly enriched.

3.4. GO and KEGG pathway analysis of 25 common proteins with significantly differential expression

The numbers of proteins with significantly differential expression and their overlap under different groups, as illustrated by Venn diagram analysis, are shown in Fig. 5 and Table 1. A Venn diagram was created to depict the overlap of differentially expressed proteins from the four groups (Control, Day 3, Day 7, and Day 14), showing that 25 were shared by the Control vs. Day 3, Control vs. Day 7, and Control vs. Day 14 (Fig. 5). The details of these 25 proteins are shown in Table 1. Among these, vimentin (Vim), albumin (Alb), inositol polyphosphate-4-phosphatase type I A (Inpp4a), Immunoglobulin Superfamily Member 1 (Igsf1), Annexin A2 (Anxa2), adhesion G protein-coupled receptor B2 (Bai2), heat shock protein family B (small) member 1 (Hspb1), Janus kinase and microtubule interacting protein 3 (Jakmip3), Superantigen (Speg), Uridine phosphorylase 1 (Upp1), BSD domain-containing 1 (Bsdc1), protein kinase AMP-activated non-catalytic subunit gamma 1 (Prkag1), potassium calcium activated channel subfamily M regulatory beta subunit 4 (Kcnmb4), Eukaryotic translation initiation factor 4E nuclear import factor 1 (Eif4enif1), ATP-binding cassette sub-family F member 1 (Abcf1), Molecule interacting with casL-like 1 (Micall1), nudix hydrolase 5 (Nudt5), ATPase secretory pathway Ca^{2+} transporting 1 (Atp2c1), GAR1 ribonucleoprotein (Gar1), exportin for tRNA (Xpot), general transcription factor IIF subunit 1 (Gtf2f1), and kinase non-catalytic C-lobe domain containing 1 (Kndc1) were upregulated, but Keratin 42 (Krt42), Keratin 10 (Krt10), and Keratin 1 (Krt1) were downregulated (Table 1).

The GO annotation and enrichment analysis of these 25 differentially expressed proteins was also implemented using KOBAS and WEGO software, respectively. GO terms with corrected *P* values less than 0.05 were considered significantly enriched. There were 1,142 GO items harvested in this study. Intermediate filament (GO: 0043209) and intermediate filament cytoskeleton (GO: 0045111) were the two most enriched items. The distribution bar charts of the biological processes, cellular components, and molecular functions are shown in Fig. 6. From the perspective of biological processes, cellular processes, metabolic processes, and pigmentation were the top three significantly enriched terms. From the perspective of molecular function, binding, catalytic, and enzyme regulator were the top three significantly enriched terms. From the perspective of cellular component, cell and cell parts were the top two significantly over-represented terms (Fig. 6).

Moreover, KOBAS software was also employed to test the statistical enrichment of these 25 differentially expressed genes in KEGG pathways. It was found that the 25 proteins were involved in 30 pathways. Fig. 7 shows the results of pathway enrichment. It clearly displays Epstein–Barr virus infection as the top enriched term (Fig. 7). Additionally, two differentially expressed genes identified in this study are known to participate in Epstein–Barr virus infection pathways. Moreover, it is worth noting that Circadian rhythm, Basal transcription factors, and Drug metabolism-other enzymes, Staphylococcus aureus infection, and the vascular endothelial growth fac-

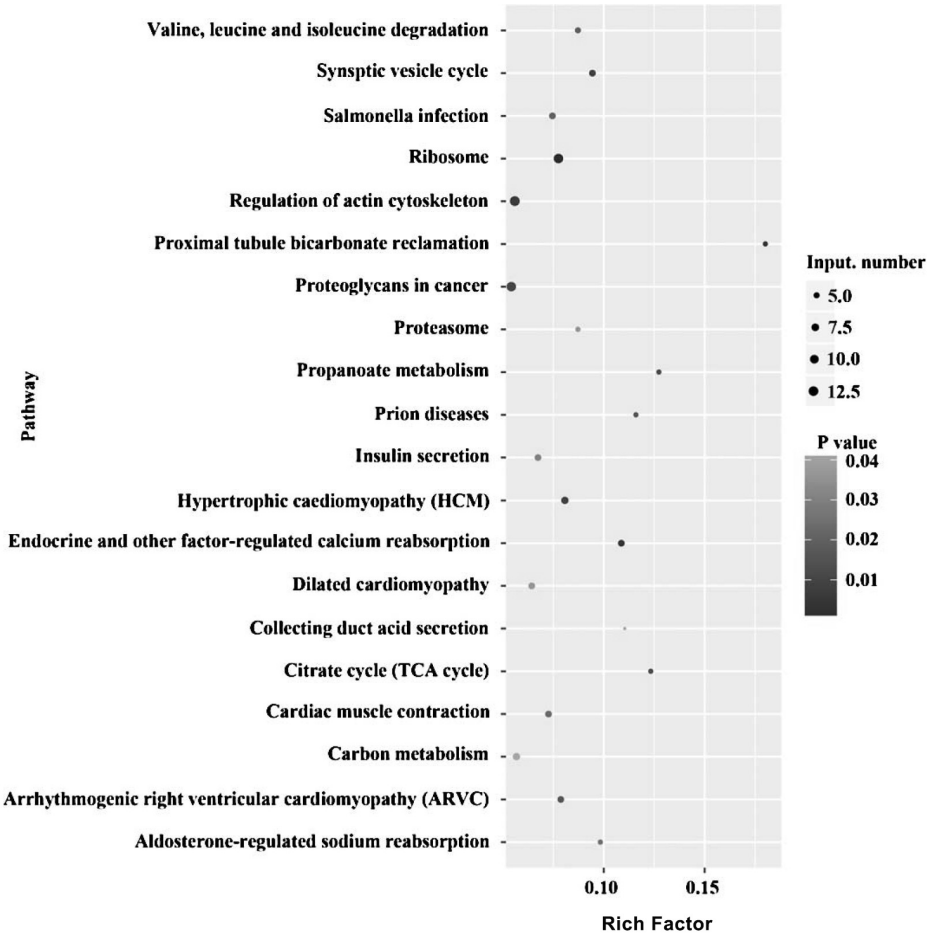

Fig. 4. Scatter diagram of enriched KEGG pathways of the 260 differentially expressed proteins identified in this study. Degree of enrichment was measured by Rich factor, *Q* value, and the number of genes enriched in one pathway. The Rich factor is the ratio of the number of differential expression genes enriched in one pathway and the GO annotation number. The greater the Rich factor value, the higher the degree of enrichment. The *Q* value is a variant of a *P* value, for which lower values equate to significant enrichment. The *Y*-axis represents the name of pathway and the *X*-axis represents the Rich factor. The point size is the number of differentially expressed genes in one pathway, and the color of the point indicates the range of the *Q* value.

tor (VEGF) signaling pathway were also found to be significantly enriched here.

3.5. PPI network analysis

The interactive protein network for the 25 differentially expressed proteins was predicted by STRING, and a total of 223 interactive proteins were searched and are represented by red arrow nodes. Black lines indicate the predicted protein directly with the differentially expressed proteins, which are represented by circular nodes. PPI network analysis found that Vim and Alb had the top two highest degrees in the constructed network (Fig. 8).

4. Discussion

In present study, iTRAQ-based quantitative proteomic analysis was performed to detect proteins in male rat hippocampus tissue after focal ischemia injury. Estrogen has been reported to have a protective effect on cerebral ischemia [30], therefore, only male rats were used to construct the focal ischemia injury model. Differential protein expression profiles from control and injured hippocampal groups were analyzed.

Two interesting results were noticed. Firstly, transcription levels of Vim, albumin, Inpp4a, Igsf1, Anxa2, Bai2, Hspb1, Jakmip3, Speg, Upp1, Bsdc1, Prkag1, Kcnmb4, Eif4enif1, Abcf1, Micall1, Nudt5, Atp2c1, Gar1, Xpot, Gtf2f1, and Kndc1 were upregulated, but Krt 1, 10, and 42 were downregulated. It has been reported that increased Upp1 expression level would potentially inhibited the expression of several pathways downstream of uridine, such as RNA/DNA and membrane synthesis, which may trigger neurodegeneration in the long-term [31]. Additionally, Adibhatla *et al.* [32] found that TNF-α and IL-1, two major inducers of Upp1 could alter the lipid peroxidation that potentiates central nervous system injury. Heat shock proteins (Hsps) are endogenous neuroprotective proteins and play a key role in neurologic disease [33], and small Hsps (sHsps) have been reported from studies of the relationships between over-expressed Hspb1 and Hspb5 (α B-crystallin) in Alzheimer's disease (AD) brains [34, 35]. Interestingly, the other members of sHsps, including Hspb2, Hspb6, and Hspb8, have also been found to be related to pathogenesis of AD [29, 36]. Meanwhile, loss of Hspb5 and Hspb2 in Tg2576 mice exacerbates behavioral deficits, suggesting a protective role [27]. *In vitro*, Hspb1, Hspb6, Hspb8,

Table 1. Significantly common differential expressed proteins in comparison of three different groups to control group

Full Name	Protein	Control	Day 3	Day 7	Day 14	Diff
vimentin	Vim	1	1.6888018	1.8868765	1.1111086	Up
albumin	Alb	1	1.9026365	1.5283766	1.8301984	Up
inositol polyphosphate-4-phosphatase type I A	Inpp4a	1	1.6200069	1.6290152	1.5800826	Up
Immunoglobulin Superfamily Member 1	Igsf1	1	2.3230176	1.8921153	1.7076355	Up
Annexin A2	Anxa2	1	2.2720585	2.044857	2.3424204	Up
Keratin 42	Krt42	1	0.3280528	0.2928025	0.383155	Down
adhesion G protein-coupled receptor B2	Bai2	1	2.2532386	2.0167047	2.1554665	Up
Keratin 10	Krt10	1	0.4665165	0.4376957	0.4944855	Down
heat shock protein family B (small) member 1	Hspb1	1	2.8599699	3.0146699	1.7950201	Up
Janus kinase and microtubule interacting protein 3	Jakmip3	1	1.6155215	1.825131	2.0279192	Up
keratin 1	Krt1	1	0.5069798	0.4425769	0.5083873	Down
Superantigen	Speg	1	3.5801003	2.7894874	3.4058149	Up
Uridine phosphorylase 1	Upp1	1	3.988925	3.988925	3.988925	Up
BSD domain-containing 1	Bsdc1	1	2.4016067	2.4016067	2.5175142	Up
protein kinase AMP-activated non-catalytic subunit gamma 1	Prkag1	1	3.1601653	3.5112872	3.2670759	Up
potassium calcium-activated channel subfamily M regulatory beta subunit 4	Kcnmb4	1	2.964934	3.1601653	3.0908423	Up
Eukaryotic translation initiation factor 4E nuclear import factor 1	Eif4enif1	1	3.5015653	3.7217987	3.6200258	Up
ATP-binding cassette sub-family F member 1	Abcf1	1	3.8264326	3.742494	3.8370565	Up
Molecule interacting with casL-like 1	Micall1	1	3.6200258	3.8477098	3.8264326	Up
nudix hydrolase 5	Nudt5	1	2.421666	1.571345	2.2973966	Up
ATPase secretory pathway Ca2+ transporting 1	Atp2c1	1	2.2783665	2.1140359	2.044857	Up
GAR1 ribonucleoprotein	Gar1	1	2.247	2.0279192	2.102346	Up
exportin for tRNA	Xpot	1	2.3817139	1.9399239	2.2657676	Up
general transcription factor IIF subunit 1	Gtf2f1	1	2.2783665	1.9507109	1.760518	Up
kinase non-catalytic C-lobe domain containing 1	Kndc1	1	2.179504	2.1140359	2.2099291	Up

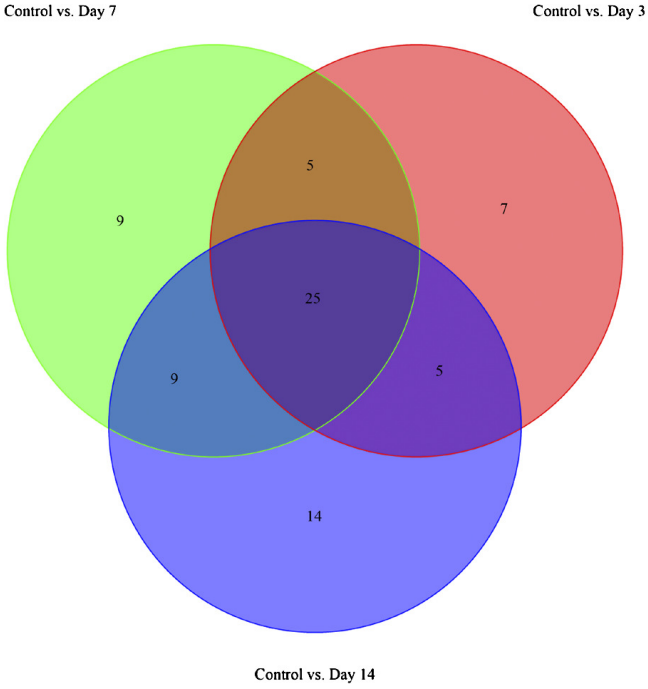

Fig. 5. Venn diagrams of differentially expressed proteins detected in the four different groups of this study. The overlap represents 25 differentially expressed proteins common to the four different groups.

and Hspb5 have been shown to play a role in the retardation of Aβ aggregation and cytotoxicity [28, 29]. Keratins are obligate heterodimer proteins that form the intermediate filament cytoskeleton of all epithelial cells [37], Krt1 and its heterodimer partner Krt 10 are major components of the intermediate filament cytoskeleton [38]. The abnormal expression of Krt 9 in cerebrospinal fluid may lead to blood brain barrier dysregulation and damage to the ubiquitin proteasome system [39].

Differentially expressed proteins were annotated by GO analysis. As expected, several GO terms were significantly enriched, including myelin sheath, cell junction, cell-substrate junction, adherens junction, focal adhesion, and cell-substrate adherens junction. Most of the differentially expressed proteins were associated with metabolic processes. Furthermore, KEGG analysis showed 260 differentially expressed genes were involved in 220 pathways. These results clearly indicate that Ribosome pathway was the top enriched term. 12 differentially expressed proteins were identified that are known to participate in metabolic pathways. Moreover, it is worth noting that proximal tubule bicarbonate reclamation, endocrine and other factor-regulated calcium reabsorption, Regulation of actin cytoskeleton, Synaptic vesicle cycle, and hypertrophic cardiomyopathy (HCM) were also significantly enriched in this study. One of the significantly enriched pathways in the differentially expressed proteins was the ribosome signaling pathway. All cells need to synthesize new proteins, in order to maintain cellular homeostasis. Ribosomes (polyribosomes), which are responsible for mediating all protein synthesis, are composed of nucleic acids and proteins. Specialized patterns of nucleic acids, rRNA and tRNA molecules, play pivotal roles for the translation of mRNA into proteins [40, 41]. The PPI network has been shown to organize all protein coding genes into a large network, which provides a better understanding of the functional organization of the proteome [42]. In the present study, a total of 223 interaction proteins were predicted and Vim and Alb had the top two highest degrees in the constructed PPI network. Vim is an intermediate filament protein, and transient ischemia has been shown to stimulate vim expression in the gerbil hippocampus and neocortex [43]. Higher

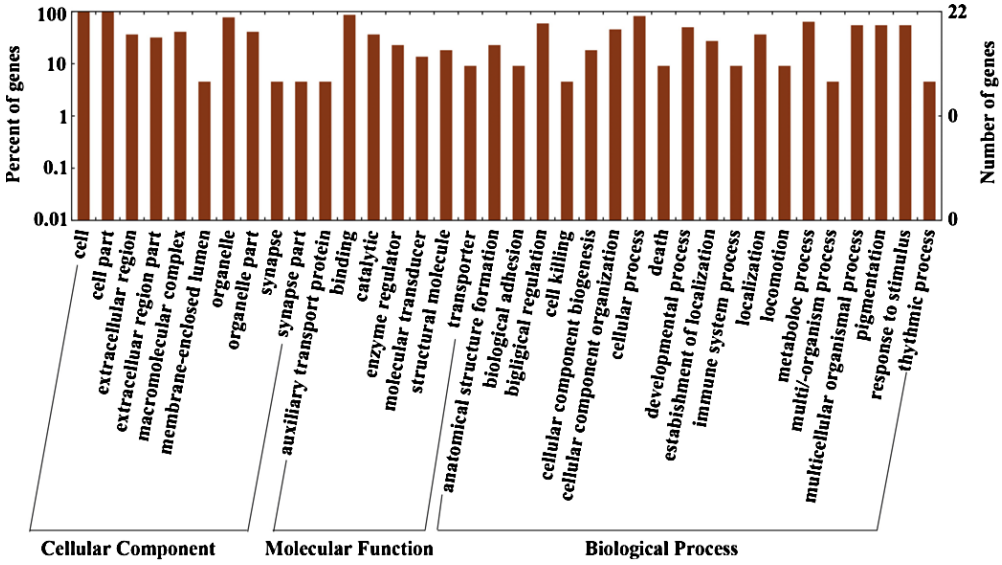

Fig. 6. GO enrichment analysis of 25 differentially expressed proteins identified in this study.

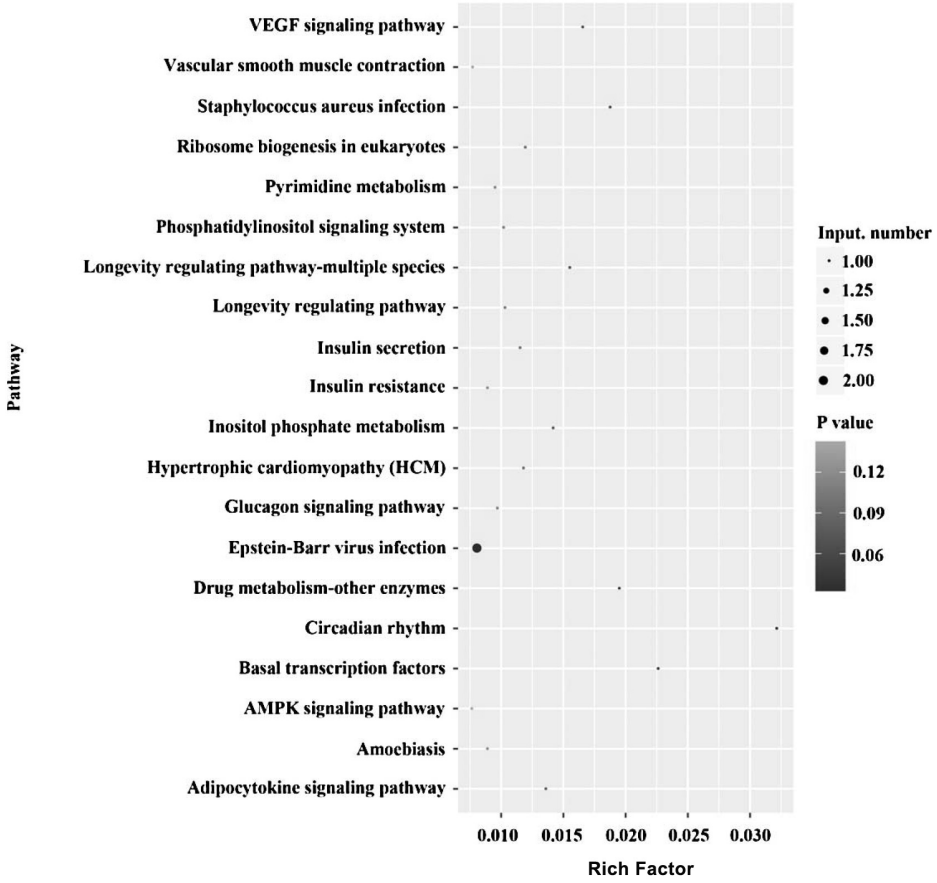

Fig. 7. Scatter diagram of enriched KEGG pathways of 25 differentially expressed proteins identified in this study. The degree of enrichment was measured by Rich factor, *Q* value, and the number of genes enriched in one pathway. The Rich factor is the ratio of the number of differentially expressed genes enriched in one pathway and the GO annotation number. The greater the value of the Rich factor, the higher the degree of enrichment. The *Q* value is a variant of a *P* value, for which lower values equate to significant enrichment. The *Y*-axis represents the name of pathway and the *X*-axis represents the Rich factor. The point size is the number of differentially expressed genes in one pathway, and the color of the point indicates the range of the *Q* value.

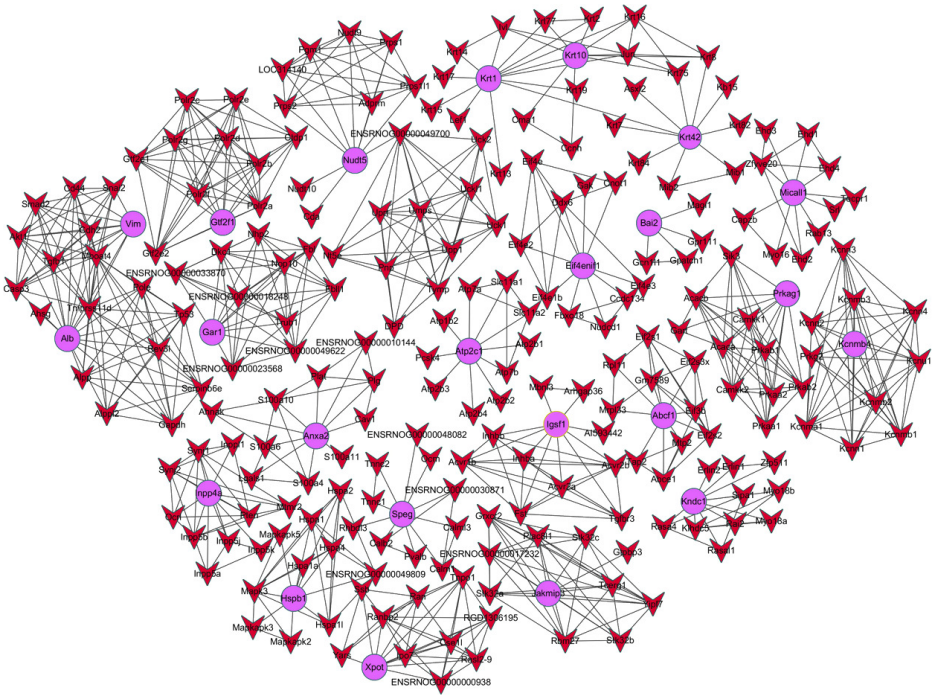

Fig. 8. A protein–protein interaction network of differentially expressed proteins. The circular nodes indicate differentially expressed proteins. Arrowed nodes stand for essential proteins predicted by STRING.

expressions of vim were associated with high neurological deficit and showed a positive correlation with brain edema [44]. In addition, Alb has been reported to have a neuroprotective effect against global ischemic brain injury in rats [45].

In conclusion, these results demonstrate that certain proteins may be involved in the process of focal ischemia injury in rats. Further, myelin sheath, cell junction, and Epstein–Barr virus infection are implicated in focal ischemia injury. Vim and Alb may also be important proteins involved in focal ischemia injury.

Acknowledgments

The authors would like to thank the Guangdong special fund for public welfare research and capacity building for their financial support. This study was supported by the Guangdong Provincial Science and Technology Department social development project (No. 2014A020212524).

Conflict of Interest

All authors declare no conflicts of interest.

References

[1] Beaglehole R, Jackson R (1992) Alcohol, cardiovascular diseases and all causes of death: a review of the epidemiological evidence. *Drug and Alcohol Review* **11(3)**, 275-289.

[2] Qi JP, Wu H, Yang Y, Wang DD, Chen YX, Gu YH, Liu T (2007) Cerebral ischemia and Alzheimer's disease: the expression of amyloid-beta and apolipoprotein E in human hippocampus. *Journal of Alzheimers Disease* **12(4)**, 335-341.

[3] Weller RO, Cohen NR, Nicoll JA (2004) Cerebrovascular disease and the pathophysiology of Alzheimer's disease. Implications for therapy. *Panminerva Medica* **46(4)**, 239-251.

[4] Pantoni L, Poggesi A, Inzitari D (2009) Cognitive decline and dementia related to cerebrovascular diseases: some evidence and concepts. *Cerebrovascular Diseases* **27(1)**, 191-196.

[5] Giorgino F, Leonardini A, Laviola L (2013) Cardiovascular disease and glycemic control in type 2 diabetes: now that the dust is settling from large clinical trials. *Annals of the New York Academy of Sciences* **1281(1)**, 36-50.

[6] Haley NJ, Sepkovic DW, Hoffmann D, Wynder EL (1985) Cigarette smoking as a risk for cardiovascular disease. Part VI. Compensation with nicotine availability as a single variable. *Clinical Pharmacology & Therapeutics* **38(2)**, 164-170.

[7] Isozumi K (2004) Obesity as a risk factor for cerebrovascular disease. *Keio Journal of Medicine* **53(1)**, 7-11.

[8] Rabkin SW, Mathewson AL, Tate RB (1978) Predicting risk of ischemic heart disease and cerebrovascular disease from systolic and diastolic blood pressures. *Annals of Internal Medicine* **88(3)**, 342-345.

[9] Wunderlich MT, Ebert AD, Kratz T, Goertler M, Jost S, Herrmann M (1999) Early neurobehavioral outcome after stroke is related to release of neurobiochemical markers of brain damage. *Stroke* **30**, 1190-1995.

[10] Patel NV, Gordon MN, Connor KE, Good RA, Engelman RW, Mason J, Morgan DG, Morgan TE, Finch CE (2005) Caloric restriction attenuates Abeta-deposition in Alzheimer transgenic models. *Neurobiology of Aging* **26(7)**, 995-1000.

[11] Zhu H, Bilgin M, Snyder M (2003) Proteomics. *Annual Review of Biochemistry* **72**, 783-812.

[12] Lankadurai BP, Nagato EG, Simpson MJ (2013) Environmental metabolomics: an emerging approach to study organism res. *Environmental Reviews* **21(3)**, 180-205.

[13] Wright PC, Biggs CA, Pham TK, Pandhal J, Ow SY, Mukherjee J, Salim M, Evans C, Noirel J (2011) Methods in Quantitative Proteomics: Setting iTRAQ on the Right Track. *Current Proteomics* **8(1)**, 17-30.

[14] Thiede B (2010) Isobaric protein and peptide quantification: perspectives and issues. *Expert Review of Proteomics* **7(5)**, 647-653.

[15] Su L, Cao L, Zhou R, Jiang Z, Xiao K, Kong W, Wang H, Deng J, Wen B, Tan F (2013) Identification of Novel Biomarkers for Sepsis Prognosis via Urinary Proteomic Analysis Using iTRAQ Labeling and 2D-LC-MS/MS. *Plos One* **8(1)**, e54237.

[16] Ow S, Cardona T, Taton A, Magnuson A, Lindblad P, Stensjo K, Wright P (2008) Quantitative shotgun proteomics of enriched heterocysts from Nostoc sp. PCC 7120 using 8-plex isobaric peptide tags. *Journal of Proteome Research* **7(4)**, 1615-1628.

[17] Pierce A, Unwin R, Evans C, Griffiths S, Carney L, Zhang L, Jaworska E, Lee C, Blinco D, Okoniewski M (2008) Eight-channel iTRAQ enables comparison of the activity of six leukemogenic tyrosine kinases. *Molecular & Cellular Proteomics* **7(5)**, 853-863.

[18] Ross PL, Huang YN, Marchese JN, Williamson B, Parker K, Hattan S, Khainovski N, Pillai S, Dey S, Daniels S (2004) Multiplexed Protein Quantitation in Saccharomyces cerevisiae Using Amine-reactive Isobaric Tagging Reagents. *Molecular & Cellular Proteomics* **3(12)**, 1154-1169.

[19] Aggarwal K, Choe LH, Lee KH (2006) Shotgun proteomics using the iTRAQ isobaric tags. *Briefings in Functional Genomics & Proteomics* **5(2)**, 112-120.

[20] Casadovela J, Martínezesteso MJ, Rodriguez E, Borrás E, Elortza F, Brumartínez R (2010) iTRAQ-based quantitative analysis of protein mixtures with large fold change and dynamic range. *Proteomics* **10(2)**, 343-347.

[21] Muth T, Keller D, Puetz SM, Martens L, Sickmann A, Boehm AM (2010) jTraqX: a free, platform independent tool for isobaric tag quantitation at the protein level. *Proteomics* **10(6)**, 1223-1225.

[22] Schwacke JH, Hill EG, Krug EL, Comte-Walters S, Schey KL (2009) iQuantitator: a tool for protein expression inference using iTRAQ. *Bmc Bioinformatics* **10(1)**, 342.

[23] Rudrabhatla P, Grant P, Jaffe H, Strong MJ, Pant HC (2010) Quantitative phosphoproteomic analysis of neuronal intermediate filament proteins (NF-M/H) in Alzheimer's disease by iTRAQ. *Faseb Journal Official Publication of the Federation of American Societies for Experimental Biology* **24(11)**, 4396-4407.

[24] Kim HS, Park MS, Lee JK, Kim HJ, Park JT, Lee MC (2011) Time Point Expression of Apoptosis Regulatory Proteins in a Photochemically-Induced Focal Cerebral Ischemic Rat Brain. *Chonnam Medical Journal* **47(3)**, 144-149.

[25] Ge P, Ma C, Wang S, Gao L, Li X, Guo G, Ma W, Yan Y (2012) Comparative proteomic analysis of grain development in two spring wheat varieties under drought stress. *Analytical & Bioanalytical Chemistry* **402(3)**, 1297-1313.

[26] Messana I, Kasicka V (2008) Analysis of peptides by separation and mass spectrometric methods. *Journal of Separation Science* **31(3)**, 425, 426.

[27] Ojha J, Karmegam RV, Masilamoni JG, Terry AV, Cashikar AG (2011) Behavioral Defects in Chaperone-Deficient Alzheimer's Disease Model Mice. *Plos One* **6(2)**, e16550.

[28] Santhoshkumar P, Sharma KK (2004) Inhibition of amyloid fibrillogenesis and toxicity by a peptide chaperone. *Molecular & Cellular Biochemistry* **267(1,2)**, 147-155.

[29] Wilhelmus MM, Boelens WC, Otte-Höller I, Kamps B, Kusters B, Maat-Schieman ML, de Waal RM, Verbeek MM (2006) Small heat shock protein HspB8: its distribution in Alzheimer's disease brains and its inhibition of amyloid-beta protein aggregation and cerebrovascular amyloid-beta toxicity. *Acta Neuropathologica* **111(2)**, 139-149.

[30] Wappler EA, Felszeghy K, Szilágyi G, Gál A, Skopál J, Mehra RD, Nyakas C, Nagy Z (2010) Neuroprotective effects of estrogen treatment on ischemia-induced behavioural deficits in ovariectomized gerbils at different ages. *Behavioural Brain Research* **209(1)**, 42-48.

[31] Saydoff JA, Liu LS, Garcia RA, Hu Z, Li D, Von Borstel RW (2003) Oral uridine pro-drug PN401 decreases neurodegeneration, behavioral impairment, weight loss and mortality in the 3-nitropropionic acid mitochondrial toxin model of Huntington's disease. *Brain Research* **994(1)**, 44-54.

[32] Adibhatla RM, Hatcher JF (2008) Altered lipid metabolism in brain injury and disorders. *Sub-cellular biochemistry* **49**, 241-268.

[33] Brownell SE, Becker RA, Steinman L (2012) The protective and therapeutic function of small heat shock proteins in neurological diseases. *Frontiers in Immunology* **3**, 74.

[34] Renkawek K, Stege GJ, Bosman GJ (1999) Dementia, gliosis and expression of the small heat shock proteins hsp27 and alpha B-crystallin in Parkinson's disease. *Neuroreport* **10(11)**, 2273-2276.

[35] Shinohara H, Inaguma Y, Goto S, Inagaki T, Kato K (1993) Alpha B crystallin and HSP28 are enhanced in the cerebral cortex of patients with Alzheimer's disease. *Journal of the Neurological Sciences* **119(2)**, 203-208.

[36] Wilhelmus MM, Otte-Höller I, Wesseling P, De Waal RM, Boelens WC, Verbeek MM (2006) Specific association of small heat shock proteins with the pathological hallmarks of Alzheimer's disease brains. *Neuropathology & Applied Neurobiology* **32(2)**, 119-130.

[37] Irvine AD, Mclean WHI (1999) Human keratin diseases: the increasing spectrum of disease and subtlety of the phenotype–genotype correlation. *British Journal of Dermatology* **140(5)**, 815-828.

[38] Roth W, Kumar V, Beer HD, Richter M, Wohlenberg C, Reuter U, Thiering S, Staratschek-Jox A, Hofmann A, Kreusch F (2012) Keratin 1 maintains skin integrity and participates in an inflammatory network in skin through interleukin-18. *Journal of Cell Science* **125(22)**, 5269-5279.

[39] Richens JL, Spencer HL, Butler M, Cantlay F, Vere K, Bajaj N, Morgan K, O'Shea P (2016) Rationalising the role of Keratin 9 as a biomarker for Alzheimer's disease. *Scientific Reports* **6**, 22962.

[40] Granneman S, Baserga SJ (2004) Ribosome biogenesis: of knobs and RNA processing. *Experimental Cell Research* **296(1)**, 43-50.

[41] Tschochner H, Hurt E (2003) Pre-ribosomes on the road from the nucleolus to the cytoplasm. *Trends in Cell Biology* **13(5)**, 255-263.

[42] Chen CY, Ho A, Huang HY, Juan HF, Huang HC (2014) Dissecting the Human Protein-Protein Interaction Network via Phylogenetic Decomposition. *Scientific Reports* **4**, 7153.

[43] Kindy MS, Bhat AN, Bhat NR (1992) Transient ischemia stimulates glial fibrillary acid protein and vimentin gene expression in the gerbil neocortex, striatum and hippocampus. *Brain Research Molecular Brain Research* **13(3)**, 199-206.

[44] LopezRodriguez AB, AcazFonseca E, Viveros MP, GarciaSegura LM (2015) Changes in cannabinoid receptors, aquaporin 4 and vimentin expression after traumatic brain injury in adolescent male mice. Association with edema and neurological deficit. *Plos One* **10(6)**, e0128782.

[45] Belayev L, Saul I, Huh PW, Finotti N, Zhao W, Busto R, Ginsberg MD (1999) Neuroprotective effect of high-dose albumin therapy against global ischemic brain injury in rats. *Brain Research* **845(1)**, 107-111.